Journal of Alloys and Compounds 525 (2012) 78–81

Contents lists available at SciVerse ScienceDirect

Journal of Alloys and Compounds

journal homepage: www.elsevier.com/locate/jallcom

Thermal expansion and solubility limits of cerium-doped lanthanum zirconates

Jinhua Zhang[a], Jishun Yu[b], Xun Cheng[a], Shu-en Hou[a,*]

[a] Engineering Research Center of Nano-Materials of Mineral of Education, Faculty of Material Science and Chemical Engineering, China University of Geosciences, Wuhan 430074, PR China

[b] State Key Laboratory of Geological Processes and Mineral Resources, Wuhan 430074, PR China

ARTICLE INFO

Article history:
Received 13 November 2011
Received in revised form 7 February 2012
Accepted 12 February 2012
Available online xxx

Keywords:
Coating materials
Precipitation
Sintering
Thermal expansion
X-ray diffraction

ABSTRACT

A series of compositions with the general formula $La_2(Zr_{2-2x}Ce_{2x})O_7$ ($0 \le x \le 0.75$) were prepared by the coprecipitation–calcination method and characterized by powder XRD. The composition of prepared ceramic materials changed from single pyrochlore structure to the mixture with pyrochlore structure and fluorite structure as x increased. The lattice parameters decreased firstly and then increased while the amount of Ce^{4+} at 298 K was increased. The thermal expansion coefficient of $La_2Zr_2O_7$ was improved by a number of Ce^{4+} adoptions at high temperature.

1. Introduction

Thermal barrier coatings (TBCs) made of low-thermal conductivity ceramics are now being used to provide thermal insulation for metallic components from the hot gas stream in gas-turbine engines used for aircraft propulsion, power generation, and marine propulsion [1]. Yttria stabilized zirconia (YSZ), is currently used as the standard material of TBCs due to its low thermal conductivity, relatively high thermal expansion coefficient and chemical inertness in combustion atmospheres [2,3]. However, the major disadvantage of YSZ is the limited operation temperature (<1473 K) for long-term application. At higher temperatures, the phase transformed gives rise to the spallation failure of the coatings [4]. On the other hand, in the next generation of advanced engines, further increase in thrust-to-weight ratio will require even higher gas temperature. This means that higher surface temperatures and larger thermal gradients are expected in advanced TBCs as compared to the conventional YSZ coating [5]. For seeking other viable candidate materials, attention has turned to the pyrochlores, $A_2^{3+}B_2^{4+}O_7$, because several zirconate pyrochlores have lower thermal conductivity than YSZ. The pyrochlores are also attractive because many are refractory up to temperatures well in excess of 1773 K and thermally stable [5,6].

$La_2Zr_2O_7$ which has a cubic pyrochlore structure was recently proposed as a promising TBCs material [7,8]. The crystal structure consists of the corner-shared ZrO_6 octahedra forming the back bone of the network and La^{3+} ions fill the holes which are formed by $6ZrO_6$ octahedra. It can largely tolerate vacancies at the La^{3+}, Zr^{4+} and O^{2-}-sites without phase transformation [9]. Both La^{3+} and Zr^{4+}-sites can be substituted by a lot of other elements with similar ionic radii in case that the electrical neutrality is satisfied, giving rise to the possibility of its thermal properties to be tailored. However, the coating of this material did not give a longer thermal cycling life than YSZ coating which might be explained by its relatively low thermal expansion coefficient and poor toughness [10–13]. The main advantages of $La_2Zr_2O_7$ as TBCs material are the low thermal conductivity and no phase transformation at high temperatures, but the lower thermal expansion coefficient limits its application. It is reported that cerium doping can improved the thermal expansion coefficient [14–17].

In this work, the phase relation studied in the $La_2(Zr_{2-2x}Ce_{2x})O_7$ ($x = 0$, 0.05, 0.10, 0.15, 0.20, 0.25, 0.50, 0.75) system and thermal expansion behavior of these solid solutions are being reported. Thermal expansion behavior, an important property from the viewpoint of mechanical integrity of such a system, will also be discussed.

2. Experimental

2.1. Sample preparation

In the present study, lanthanum oxide, cerium nitrate hexahydrate and zirconium oxychloride octahydrate were chosen as the reactants. The Ce^{4+}-doped $La_2Zr_2O_7$ was prepared by coprecipitation–calcination method [13]. Firstly, the lanthanum oxide was dissolved in nitric acid, zirconium oxychloride octahydrate and cerium nitrate hexahydrate were dissolved in distilled water, respectively. For the

* Corresponding author. Tel.: +86 27 67885168.
E-mail address: shenhou@cug.edu.cn (S. Hou).

0925-8388/$ – see front matter © 2012 Elsevier B.V. All rights reserved.
doi:10.1016/j.jallcom.2012.02.077

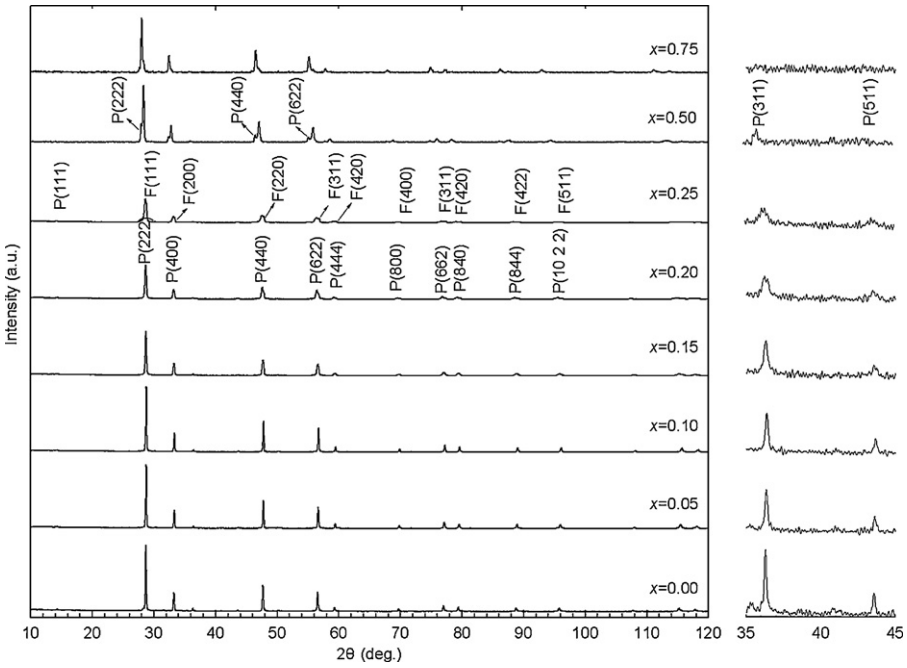

Fig. 1. XRD patterns of different compositions in $La_2(Zr_{2-2x}Ce_{2x})O_7$ at 298 K.

preparation of $La_2(Zr_{2-2x}Ce_{2x})O_7$ ($x = 0, 0.05, 0.10, 0.15, 0.20, 0.25, 0.50, 0.75$) ceramic powders, these solutions were mixed in appropriate proportions and stirred for 30 min. The precursor solution was slowly added to ammonia solution with pH 10, with stirring, to obtain gel-like precipitates, which were then centrifugated and washed with distilled water. After that, the precipitates were washed and centrifugated with absolute ethyl alcohol for 2 times and with normal propyl alcohol for 1 time. The washed precipitates were dried at 393 K for 12 h and the precursor powders were gained. The powders were calcined at 1473 K for 2 h.

2.2. X-ray diffraction

X-ray diffraction (XRD) data collection was performed with a Philips X'Pert PRO diffratometer with Ni filtered Cu Kα radiation (λ = 0.154056 nm). For lattice thermal expansion studies, the XRD patterns of samples were recorded from $2\theta = 10–120^\circ$, in the temperature range 298–1673 K on a Philips X'Pert PRO unit equipped with Anton Paar HTK attachment with the Pt sample holder at the vacuum (6.3 Pa). The temperature was controlled by a PID-type temperature controller unit to with in ±1 K during the XRD measurements. The samples were heated by the rate of 10 K/min and equilibrated for 5 min at each temperature before XRD measurement. In order to determine the solubility limits, the lattice parameters were refined by a least squares method.

3. Results and discussion

The XRD patterns of all the products in $La_2(Zr_{2-2x}Ce_{2x})O_7$ ($0.00 \le x \le 0.75$) were recorded in Fig. 1 and analyzed. When $x \le 0.20$, all the products were found to have pyrochlore super-type lattice, which was characterized by the presence of typical superlattice peaks at $2\theta \approx 37^\circ$ (3 3 1), 45° (5 1 1) (using Cu Kα as radiation source). These two peaks could help us to distinguish the fluorite and pyrochlore structures. As x increased to 0.25, two different structures of pryochlore type lattice and fluorite type lattice could be observed. In the series of $La_2(Zr_{2-2x}Ce_{2x})O_7$, $La_2(Zr_{1.4}Ce_{0.6})O_7$ was a mixture of pyrochlore and fluorite. The main phase in $La_2(Zr_{1.4}Ce_{0.6})O_7$ was $La_2Zr_2O_7$ with a small solubility of $La_2Ce_2O_7$, and this phase kept pyrochlore structure. The second phase was a solid solution with fluorite structure [14,15,17]. As $x = 0.5$, two different structures were observed too, and the major phase showed fluorite structure. As $x = 0.75$, the structure transformed into fluorite. The ionic radius of Ce^{4+} (0.092 nm) was larger than that of Zr^{4+} (0.072 nm) [18], so as $x > 0.25$, $La_2(Zr_{2-2x}Ce_{2x})O_7$ did not form complete solid solutions.

The cell parameters for the each solid solution, along with both the end members were calculated. The variation of lattice parameter as a function of x was included in Table 1. The variation of lattice parameter of these solid solutions increased on incorporation of Ce^{4+} as also shown in Fig. 2. There was a decrease in lattice parameter as the x value increases to 0.10, then a rapid increase could be found in lattice parameter up to 0.20.

The composition of the products obtained after sintered process could be generalized as $La_2(Zr_{2-2x}Ce_{2x})O_7$ considering the possible aerial oxidation of Ce^{3+} ions to Ce^{4+} [19]. The ionic radii difference between Ce^{4+} (0.097 nm in 8-fold coordination) and La^{3+} (0.105 nm in 8-fold coordination) was near to the ionic radii difference between Ce^{4+} (0.092 nm in 6-fold coordination) and Zr^{4+} (0.072 nm in 6-fold coordination) [19], so it is possible that both La^{3+} and Zr^{4+} can be replaced by Ce^{4+}. If La^{3+} was replace by Ce^{4+}, the lattice parameter would be decreased, and if Zr^{4+} was replaced by Ce^{4+}, the lattice parameter would be increased. Thus, it could be inferred that the initial decrease in lattice parameter was due to the relatively smaller ionic radius difference between La^{3+} and Ce^{4+}

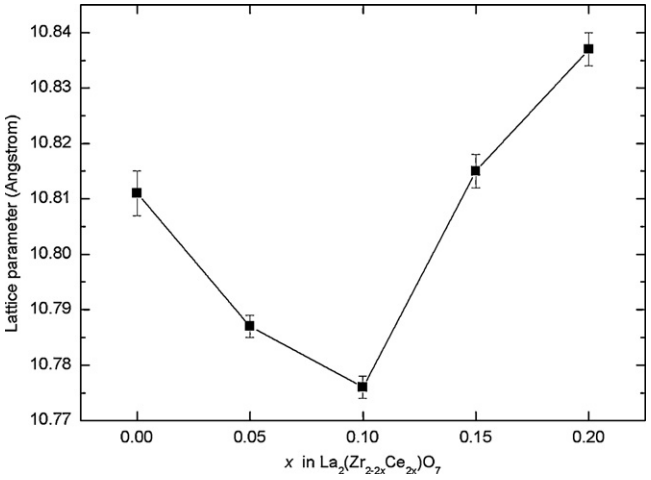

Fig. 2. Lattice parameter as a function of x in $La_2(Zr_{2-2x}Ce_{2x})O_7$ at 298 K.

Table 1
Lattice parameters (Å) at different temperature for different compositions in $La_2(Zr_{1-x}Ce_x)_2O_7$.

Temperature (K)	0.00	0.05	0.10	0.15	0.20
298	10.811(4)	10.787(2)	10.776(2)	10.815(3)	10.837(3)
473	10.828(4)	10.806(2)	10.793(2)	10.829(2)	10.851(3)
673	10.848(4)	10.830(2)	10.819(3)	10.851(2)	10.869(3)
873	10.869(4)	10.850(2)	10.841(2)	10.873(3)	10.898(3)
1073	10.892(3)	10.872(2)	10.866(2)	10.894(3)	10.919(2)
1273	10.910(4)	10.899(2)	10.899(2)	10.926(3)	10.945(2)
1323	10.915(4)	10.906(2)	10.907(2)	10.930(3)	10.951(3)
1373	10.921(4)	10.912(2)	10.914(2)	10.938(3)	10.962(3)
1423	10.927(4)	10.918(2)	10.921(2)	10.946(3)	10.964(3)
1473	10.933(4)	10.924(2)	10.926(2)	10.956(3)	10.970(3)
1523	10.939(3)	10.931(2)	10.932(2)	10.960(3)	10.980(3)
1573	10.945(4)	10.936(2)	10.937(2)	10.966(2)	10.986(3)
1623	10.951(4)	10.942(2)	10.942(2)	10.969(3)	10.991(2)
1673	10.957(4)	10.947(2)	10.948(2)	10.970(3)	10.993(3)
Thermal expansion coefficient ($\times 10^{-6}$ K^{-1}) (298–1673 K)	9.82	10.79	11.61	10.42	10.47

ions and the ionic radii of La^{3+} is larger than that of Ce^{4+}. Based on the relative ionic size considerations, we could explain the increase in the lattice parameter as $x > 0.10$.

The observation of the pyrochlore phase throughout the homogeneity range could be attributed to the range of r_A/r_B (r_A and r_B are the ionic radii of the A and B cations respectively) ratio which varied from 1.47 (in $La_2Zr_2O_7$) to 1.41 (in $La_2(Zr_{1.6}Ce_{0.4})O_7$), within the limiting radii ratio required for the stabilization of pyrochlore structure. An interesting observation was that the intensity of characteristic pyrochlore super-structure peaks systematically diminished and the full width at half-maximum of other peaks systematically increased from $La_2Zr_2O_7$ to $La_2(Zr_{1.6}Ce_{0.4})O_7$ in $La_2(Zr_{2-2x}Ce_{2x})O_7$ series. This observation can also be explained based on the radii ratio. As the radii ratio decreased, the pyrochlore lattice tended to get converted to defect-fluorite lattice [20]. As x value increased to 0.25, besides the pyrochlore super-structure, the fluorite-type structure had been shown by the XRD pattern, which had also proven it.

The lattice thermal expansion behavior of all the samples which had nominal composition $La_2(Zr_{2-2x}Ce_{2x})O_7$ were also investigated. The XRD patterns recorded for each sample at different temperatures were refined to get the lattice parameters as a function of temperature (Table 1). The variation of lattice parameters as a function of temperature was shown in Fig. 3. It could be seen that the lattice parameter increased linearly with increasing temperature for all the composition. Few typical XRD patterns of $La_2(Zr_{1.8}Ce_{0.2})O_7$ at different temperatures were shown in Fig. 4. There was no difference among the XRD patterns, implying that $La_2(Zr_{2-2x}Ce_{2x})O_7$ ($x \leq 0.20$) was thermally stable in the temperature range of interest for TBC applications (<1673 K). In zirconia-based materials, below 1473 K, stabilizers such as CeO_2 and Y_2O_3 either precipitate from the material or at 1673 K, selectively diffuse into cubic zirconia giving rise to the instabilization of the coating [21].

The average lattice thermal expansion coefficients, α_a (298–1673 K) were also included in Table 1. Lattice thermal expansion coefficients were measured in the range of 298–1673 K. The variation of α_a as a function of temperatures were shown in Fig. 5. For comparison, the thermal expansion coefficients of both the bond coat and 8YSZ were also indicated in Fig. 5 [21]. It could be seen that part of Ce^{4+} replaced Zr^{4+} into $La_2Zr_2O_7$, which could improve the thermal expansion coefficient and the thermal expansion coefficient of $La_2(Zr_{1.8}Ce_{0.2})O_7$ was larger than 8YSZ at high temperature (1473–1673 K). Compared to the bond coat, the thermal expansion coefficients of $La_2(Zr_{2-2x}Ce_{2x})O_7$ ($0 < x \leq 0.20$) were also lower. The main advantages of $La_2(Zr_{2-2x}Ce_{2x})O_7$ ($0 < x \leq 0.20$) as TBC material were the high thermal expansion coefficient, low thermal conductivity, and no phase transformation at high temperature. The investigation of this work indicated that this is a very promising TBC candidate for applications up to 1673 K.

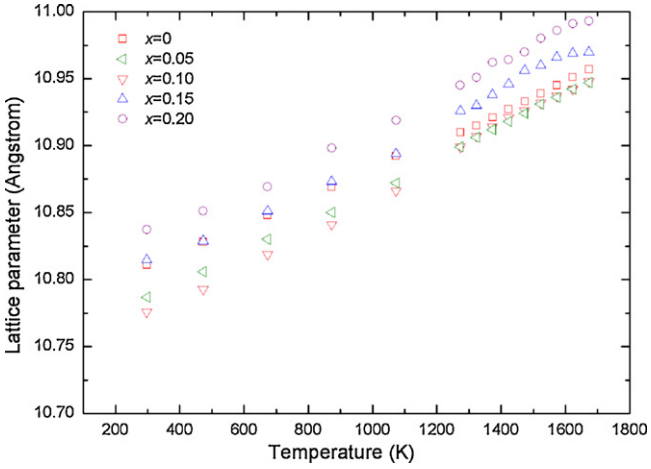

Fig. 3. Lattice parameter of $La_2(Zr_{2-2x}Ce_{2x})O_7$ vs. temperatures.

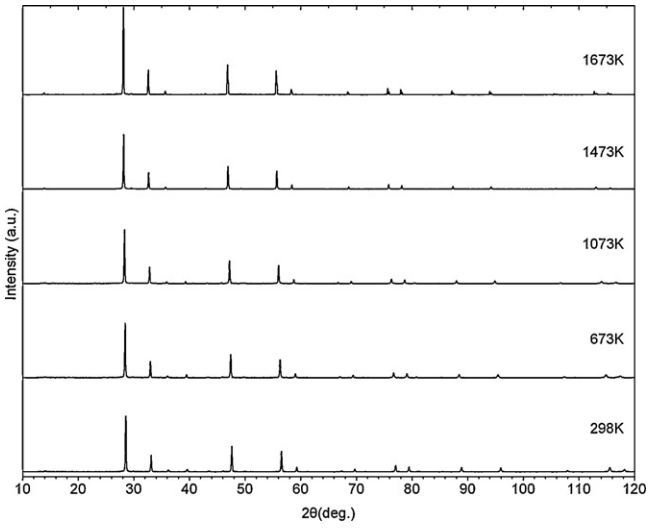

Fig. 4. High temperature XRD patterns of $La_2(Zr_{1.8}Ce_{0.2})O_7$ at different temperatures.

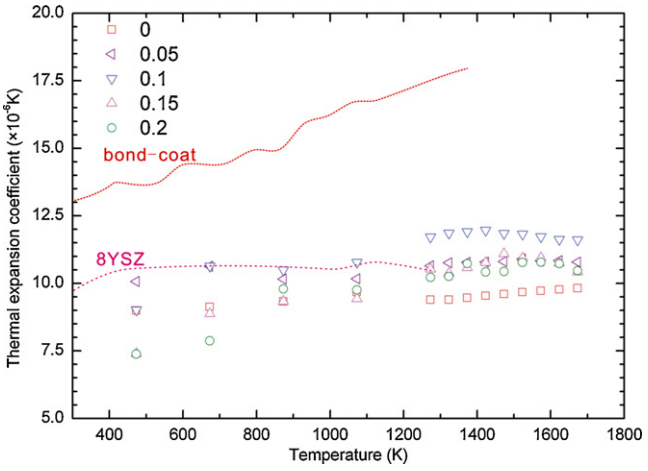

Fig. 5. Thermal expansion coefficients of $La_2(Zr_{2-2x}Ce_{2x})O_7$ vs. temperature.

4. Conclusions

(1) Lanthanum zirconate and Ce^{4+}-doped $La_2(Zr_{2-2x}Ce_{2x})O_7$ ($x = 0.05$, 0.10, 0.15, 0.20, 0.25, 0.50, 0.75) ceramics were synthesized by the coprecipitation–calcination method. When $x \geq 0.25$, the composition of the prepared ceramic materials changed from single pyrochlore structure to the mixture of pyrochlore structure and fluorite structure.

(2) The effect of doping concentration of Ce^{4+} on the lattice parameters was studied. The lattice parameters decreased firstly and then increased while the amount of Ce^{4+} was increased. $La_2(Zr_{1.80}Ce_{0.20})O_7$ powder had a minimum value of lattice parameter (10.776(2) Å) at 298 K.

(3) The thermal expansion coefficients of $La_2Zr_2O_7$ were improved by a number of Ce^{4+} adoptions at high temperature, but then deteriorated as the amount of Ce^{4+} was increased continually. The optimum amount of Ce^{4+} was about $x = 0.10$.

References

[1] N.P. Padture, M. Gell, E.H. Jordan, Science 12 (2002) 280–284.
[2] X. Ma, F. Wu, J. Roth, M. Gell, E.H. Jordan, Surface & Coating Technology 201 (2006) 4447–4452.
[3] J.I. Eldridge, C.M. Spuckler, K.W. Street, J.R. Markham, in: H.T. Lin, M. Singh (Eds.), The 26th Annual Conference on Composites, Advanced Ceramics, Materials, and Structures B: Ceramic Engineering and Science Proceedings, The American Ceramic Society, Cocoa Beach, FL, 2002, pp. 417–430.
[4] D.R. Clarke, S.R. Philpot, Materials Today 5 (2005) 22–29.
[5] X.Q. Cao, R. Vassen, D. Stöver, Journal of European Ceramic Society 24 (2004) 1–10.
[6] R. Baßen, M.O. Jarligo, T. Steinke, D.E. Mack, D. Stöver, Surface & Coating Technology 205 (2010) 938–942.
[7] B. Saruhan, P. Francois, K. Fritscher, U. Schulz, Surface & Coating Technology 182 (2004) 175–183.
[8] Z. Xu, X. Zhong, J. Zhang, Y. Zhang, X. Cao, L. He, Surface & Coating Technology 202 (2008) 4714–4720.
[9] R.S. Roth, Journal of Research of the National Institute of Standards and Technology 56 (1956) 17.
[10] Z. Xu, L. He, X. Zhong, J. Zhang, X. Chen, H. Ma, X. Cao, Journal of Alloys and Compounds 480 (2009) 220–224.
[11] H. Zhang, S. Liao, X. Dang, S. Guan, Z. Zhang, Journal of Alloys and Compounds 509 (2011).
[12] H. Zhang, Q. Xu, F. Wang, L. Liu, Y. Wei, X. Chen, Journal of Alloys and Compounds 475 (2009) 624–628.
[13] J. Wang, S. Bai, H. Zhang, C. Zhang, Journal of Alloys and Compounds 476 (2009) 89–91.
[14] X.Q. Cao, R. Vassen, F. Tietz, D. Stöver, Journal of European Ceramic Society 26 (2006) 247–252.
[15] X.Q. Cao, J.Y. Li, X.H. Zhong, J.F. Zhang, Y.F. Zhang, R. Vassen, D. Stöver, Materials Letters 62 (2008) 2667–2669.
[16] A.K. Tyagi, B.R. Ambekar, M.D. Mathews, Journal of Alloys and Compounds 337 (2002) 277–281.
[17] Z.H. Xu, L.M. He, Y. Zhao, R.D. Mu, S.M. He, X.Q. Cao, Journal of Alloys and Compounds 491 (2010) 729–736.
[18] S. Dixon, J. Marr, E.E. Lachowski, J.A. Gard, F.P. Glasser, Materials Research Bulletin 15 (1980) 1811–1816.
[19] B.P. Mandal, R. Shukla, S.N. Achary, A.K. Tyagi, Inorganic Chemistry 49 (2010) 10415–10421.
[20] B.P. Mandal, A.K. Tyagi, Journal of Alloys and Compounds 437 (2007) 260–263.
[21] X.Q. Cao, R. Vassen, W. Fischer, F. Tietz, W. Jungen, D. Stöver, Advanced Materials 15 (2003) 1438–1442.